

**Carbon cycle response to temperature overshoot beyond 2 °C – an analysis of CMIP6 models**

I. Melnikova<sup>1,2</sup>, O. Boucher<sup>1</sup>, P. Cadule<sup>1</sup>, P. Ciais<sup>3</sup>, T. Gasser<sup>4</sup>, Y. Quilcaille<sup>4</sup>, H. Shiogama<sup>2</sup>, K. Tachiiri<sup>2,5</sup>, T. Yokohata<sup>2</sup> and K. Tanaka<sup>2,3</sup>

<sup>1</sup> Institut Pierre-Simon Laplace, Sorbonne Université / CNRS, France

<sup>2</sup> Center for Global Environmental Research (CGER), National Institute for Environmental Studies (NIES), Japan

<sup>3</sup> Laboratoire des Sciences du Climat et de l'Environnement (LSCE), Commissariat à l'énergie atomique et aux énergies alternatives (CEA CNRS UVSQ), Gif-sur-Yvette, France

<sup>4</sup> International Institute for Applied Systems Analysis (IIASA), Austria

<sup>5</sup> Research Institute for Global Change, Japan Agency for Marine-Earth Science and Technology, Japan

**Contents of this file**

Tables S1 to S2 and figures S1 to S16

**Introduction**

This supporting information contains two tables and sixteen figures.

**Table S1.** Ensemble members used in each experiment and each model

ESM	IPSL-CM6A-LR	CNRM-ESM2-1	CanESM5	MIROC-ES2L	UKESM1-0-LL	CESM2-WACCM
<b>piControl</b>	rlilp1f1	rlilp1f2 (parent to r2..)	rlilp1f1, rlilp2f1	rlilp1f2	rlilp1f2 (parent to r4..)	rlilp1f1
<b>historical</b>	rlilp1f1 (1910)	r2ilp1f2 (1883)	rlilp1f1 (5201)	rlilp1f2 (1850)	r4ilp1f2 (1960)	rlilp1f1 (55)
<b>ssp534-over</b>	rlilp1f1	r2ilp1f2	rlilp1f1	rlilp1f2	r4ilp1f2	rlilp1f1
<b>ssp585</b>	rlilp1f1	r2ilp1f2	rlilp1f1	rlilp1f2	r4ilp1f2	rlilp1f1
<b>hist-bgc</b>	rlilp1f1 (1910)	rlilp1f2 (1850)	rlilp2f1 (5550)	rlilp1f2 (1850)	r4ilp1f2 (1960)	
<b>ssp534-over-bgc</b>	rlilp1f1	rlilp1f2	rlilp2f1	rlilp1f2	r4ilp1f2	
<b>ssp585-bgc</b>	rlilp1f1	rlilp1f2	rlilp2f1	rlilp1f2	r4ilp1f2	

Values in the bracket indicate the branching year from the piControl.

**Table S2.** Cumulative carbon uptake by land and ocean (GtC) by the year 2100 in this study and when the  $\beta$  and  $\gamma$  are fixed as means of the five years corresponding to the peak of CO<sub>2</sub> concentration (2060-2065) and temperature (vary among models).

	IPSL-CM6A-LR	CNRM-ESM2-1	CanESM5	UKESM1-0-LL	MIROC-ES2L
<b>This study:</b>					
$\Delta C_{\text{land}}$	266.8	529.7	226.6	78.9	231.1
$\Delta C_{\text{ocean}}$	349.1	356.0	299.9	305.2	496.7
$\Delta C_{\text{Total}}$	<b>615.9</b>	<b>885.7</b>	<b>526.5</b>	<b>384.1</b>	<b>727.9</b>
<b>Const <math>\beta</math> and <math>\gamma</math> after the peak:</b>					
$\Delta C_{\text{land}}$	141.8	224.5	156.1	13.6	119.3
$\Delta C_{\text{ocean}}$	214.2	576.5	199.2	187.3	197.7
$\Delta C_{\text{Total}}$	<b>356.0</b>	<b>801.0</b>	<b>355.3</b>	<b>200.9</b>	<b>317.0</b>

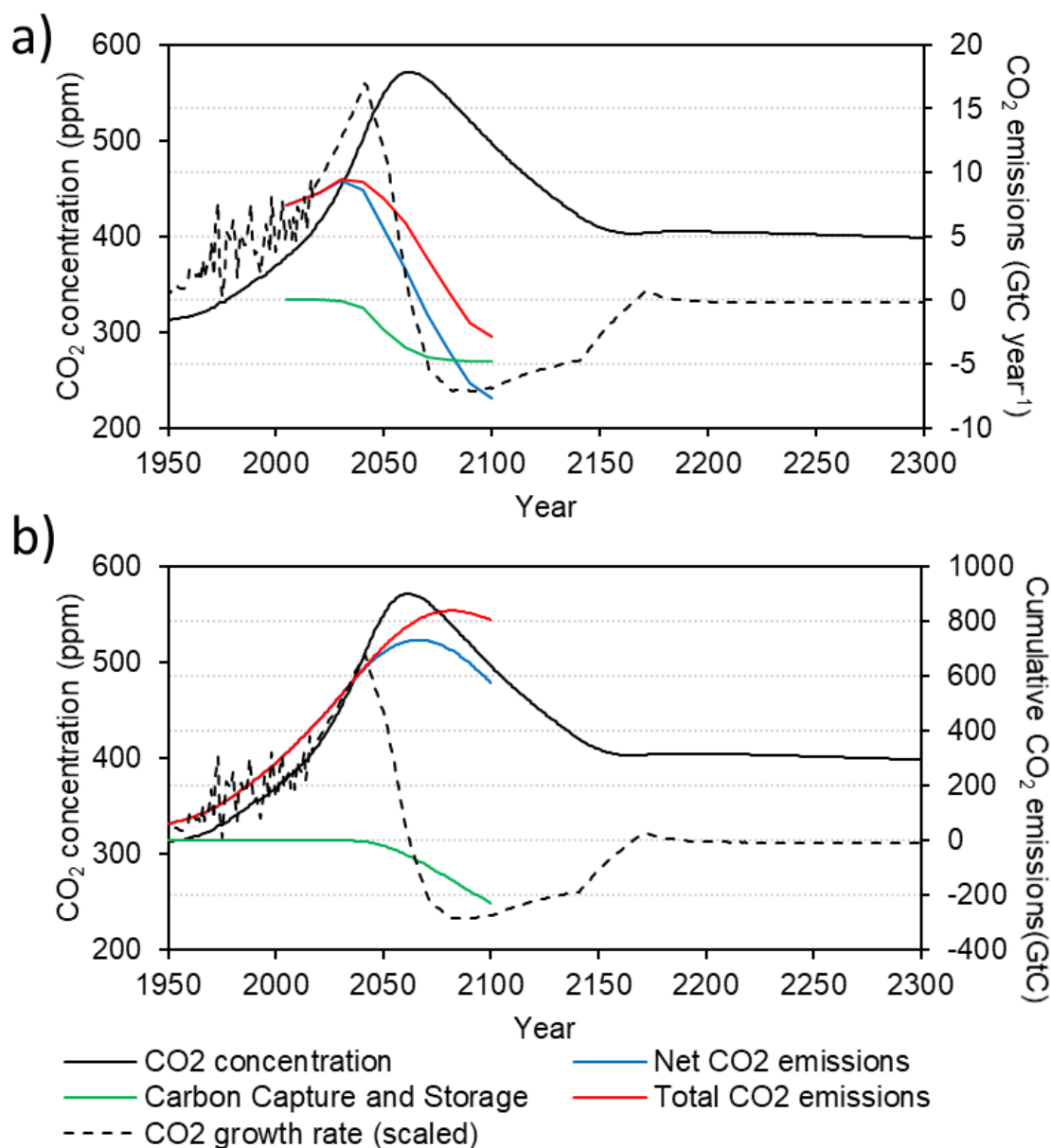


**Figure S1.** Time series of CO<sub>2</sub> concentration (ppm), CO<sub>2</sub> growth rate (scaled) and corresponding (a) CO<sub>2</sub> emissions (GtC year<sup>-1</sup>) and (b) cumulative CO<sub>2</sub> emissions (GtC) by REMIND-MAgPIE from input4MIP for SSP-5-3.4-OS experiment. Emission data are from the Integrated Assessment Modeling Consortium & International Institute for Applied Systems Analysis (IIASA) database at <https://tntcat.iiasa.ac.at/>. Fossil fuel emission data prior year 2005 are from GCB2019 data set.

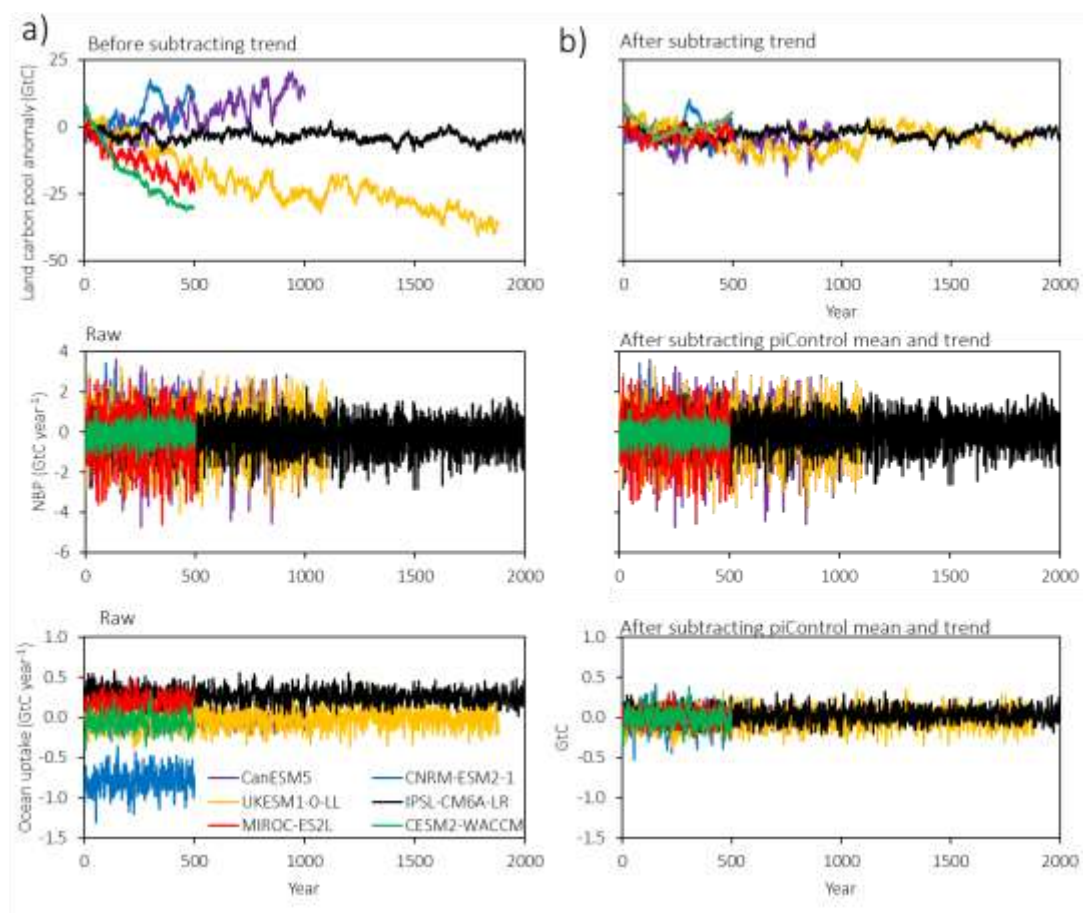


**Figure S2.** Time series of changes in global land biomass, land (NBP), and ocean carbon uptakes in the piControl experiment before (a) and after (b) pre-processing.

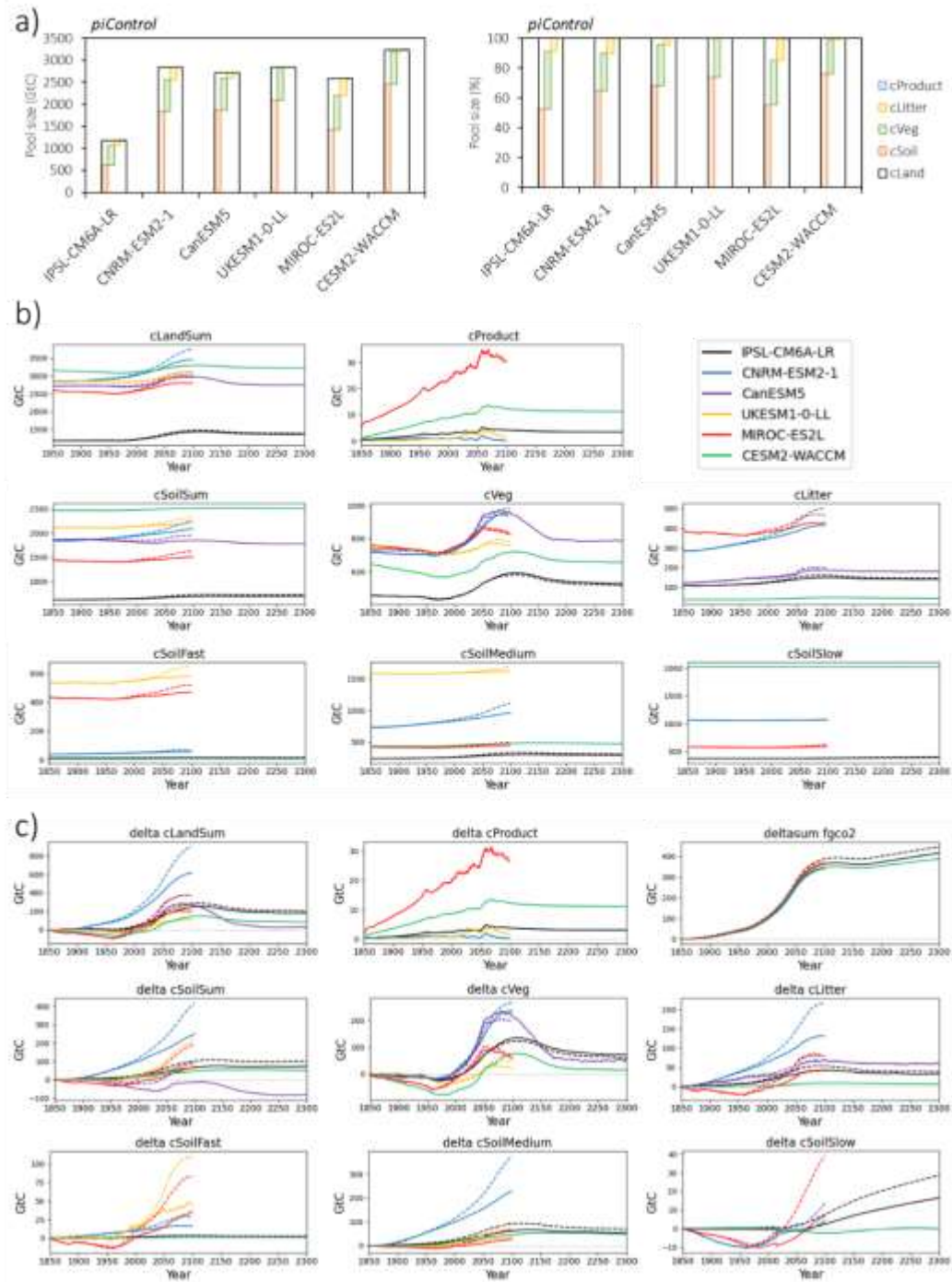


**Figure S3.** Mean land carbon pool sizes in piControl by six earth system models in fully and biogeochemically coupled simulations of SSP5-3.4-OS experiment (a). Land carbon storage (cLandSum) is calculated as a sum of vegetation, soil, litter, and product pools. Soil pool (cSoilSum) is calculated as a sum of the fast, medium, and slow soil pools, where such data are available. Time series in land carbon pools (b) and anomalies of land carbon pools and cumulative ocean flux from piControl (c). Solid lines indicate COU run, and dashed lines indicate BGC run.

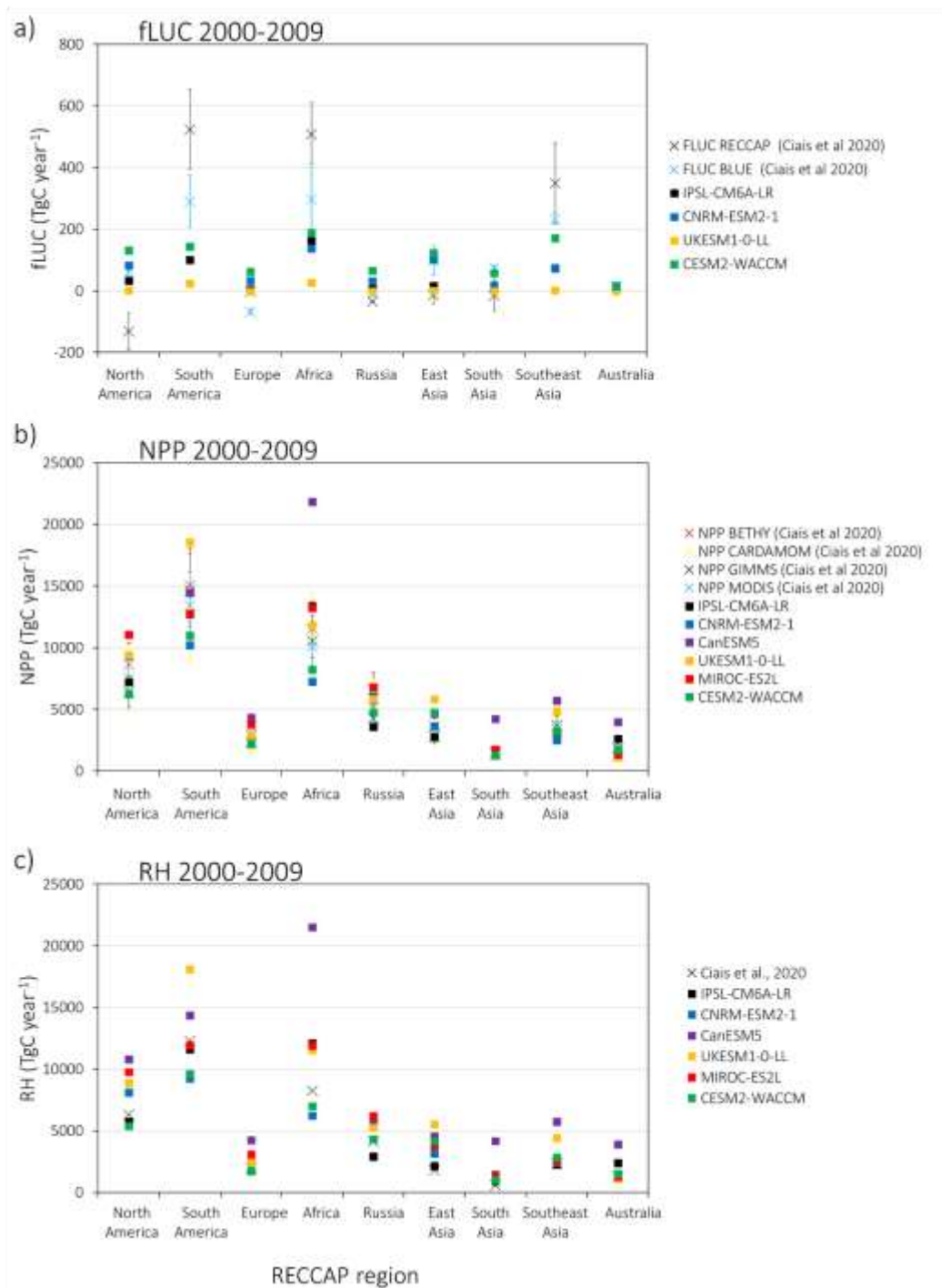


**Figure S4.** An evaluation of Earth system models (ESMs) against observational data set by Ciais et al. (2020). (a) fLUC, (b) NPP and (c) RH with associated uncertainty at nine RECCAP regions in 2000-2009.

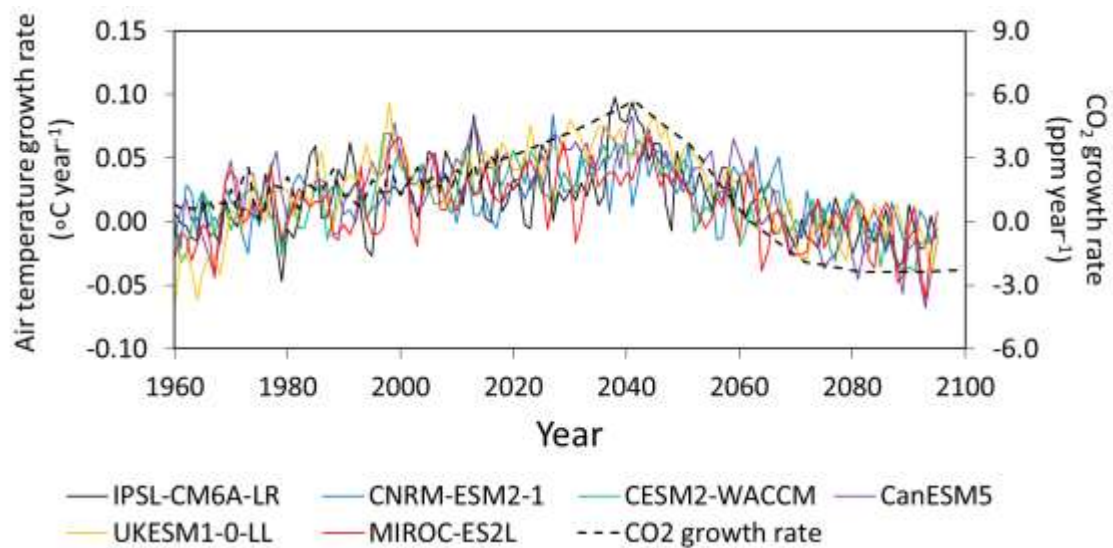


**Figure S5.** Time series of the growth rate of air temperature and by six earth system models and CO<sub>2</sub> concentration in SSP5-3.4-OS experiment. Rates of change in air temperature are given as a 10-year moving average.



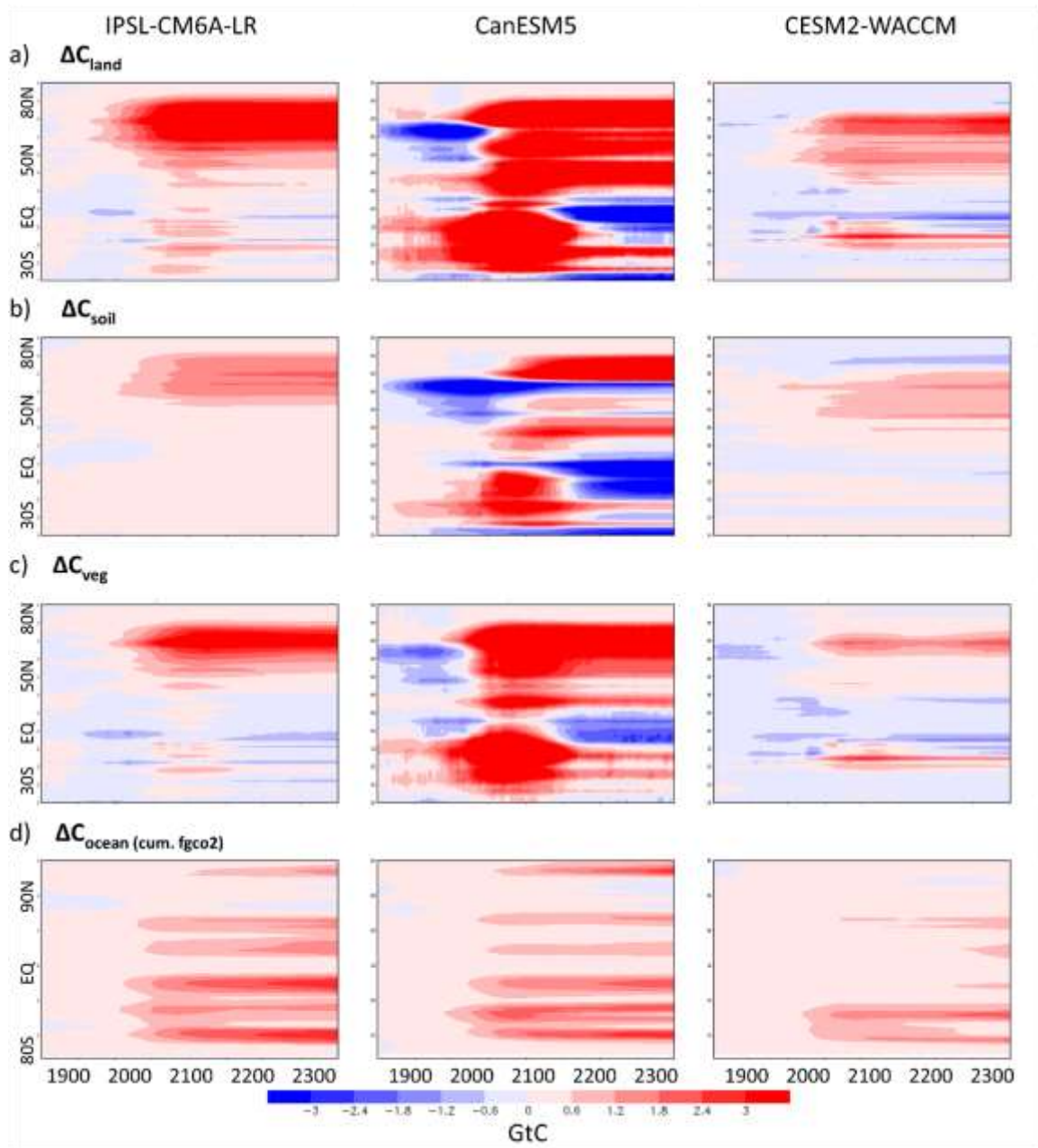


**Figure S6.** The spatiotemporal variation of zonal cumulative (a)  $\Delta C_{\text{land}}$ , (b)  $\Delta C_{\text{soil}}$ , (c)  $\Delta C_{\text{veg}}$ , and  $\Delta C_{\text{ocean}}$  (GtC) for CanESM5, CESM2-WACCM, and IPSL-CM6A-LR in 1900-2300 under SSP5-3.4-OS pathway.  $\Delta C_{\text{ocean}}$  is calculated from cumulative flux fgco2 over time.



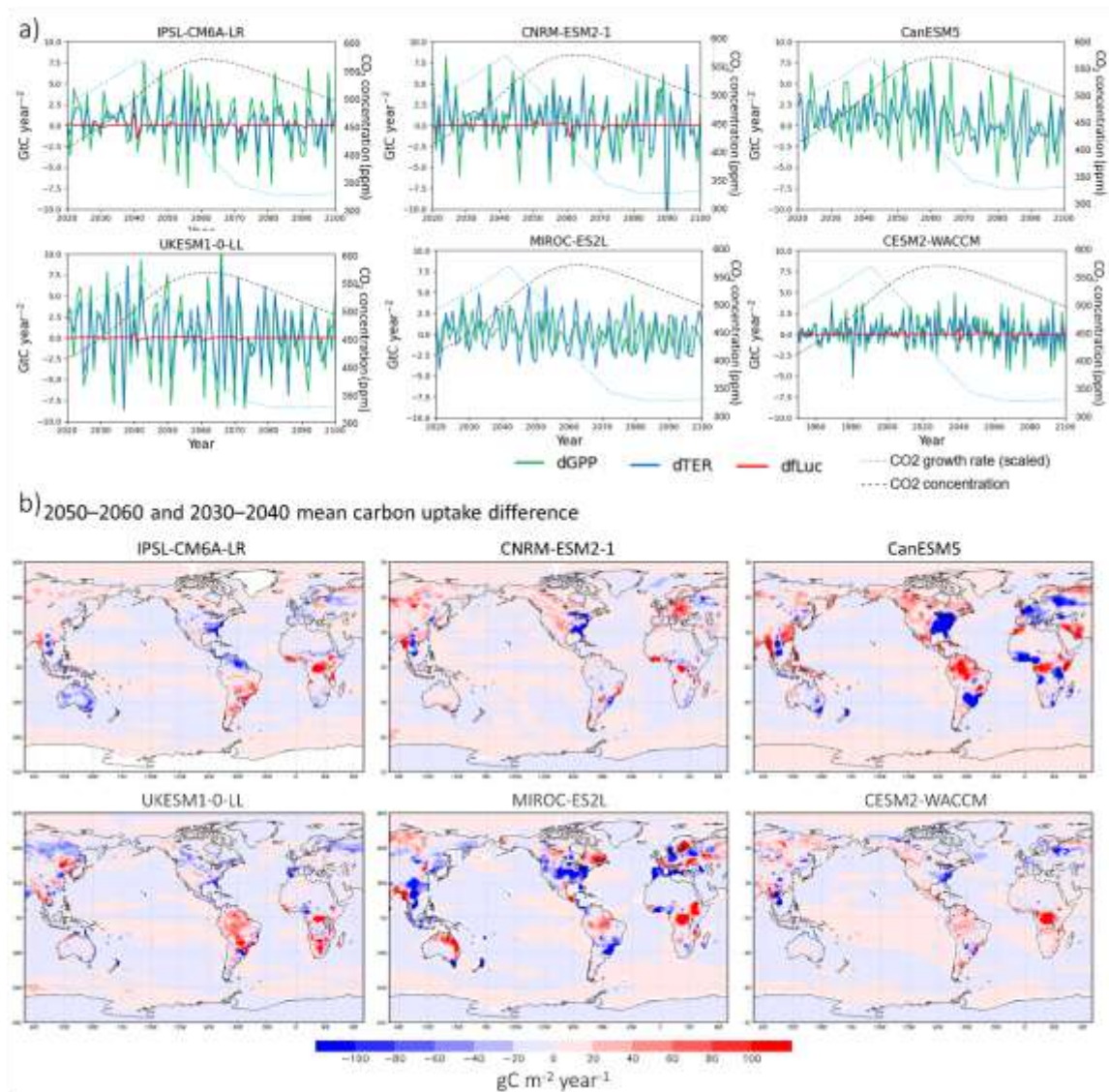


**Figure S7.** Panel (a) shows the time series of the derivatives of GPP, TER, fLUC ( $\text{GtC year}^{-2}$ ), CO<sub>2</sub> concentration (ppm), and scaled CO<sub>2</sub> growth rate. fLUC is missing in CanESM5 and MIROC-ES2L because model teams did not provide this variable. Panel (b) shows the spatial variation of the difference between the mean ocean and land uptakes (NBP and fgco<sub>2</sub>) in 2050–2060 and 2030–2040. Positive values indicate an increase in carbon uptake in a later period.

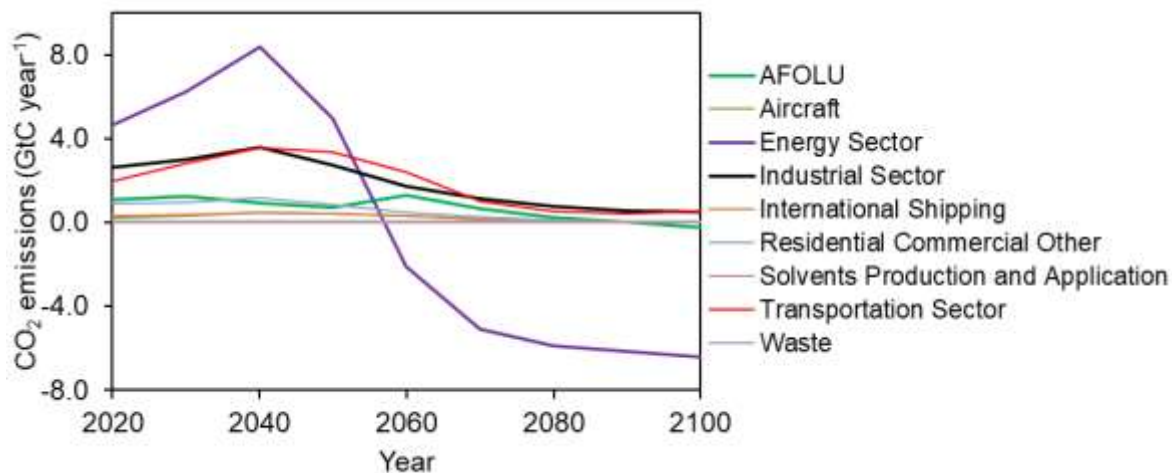


**Figure S8.** Time series of changes in CO<sub>2</sub> emissions simulated by REMIND-MAGPIE under SSP5-3.4-OS pathway.

#### 2050–2060 and 2030–2040 mean bioenergy cropland area difference

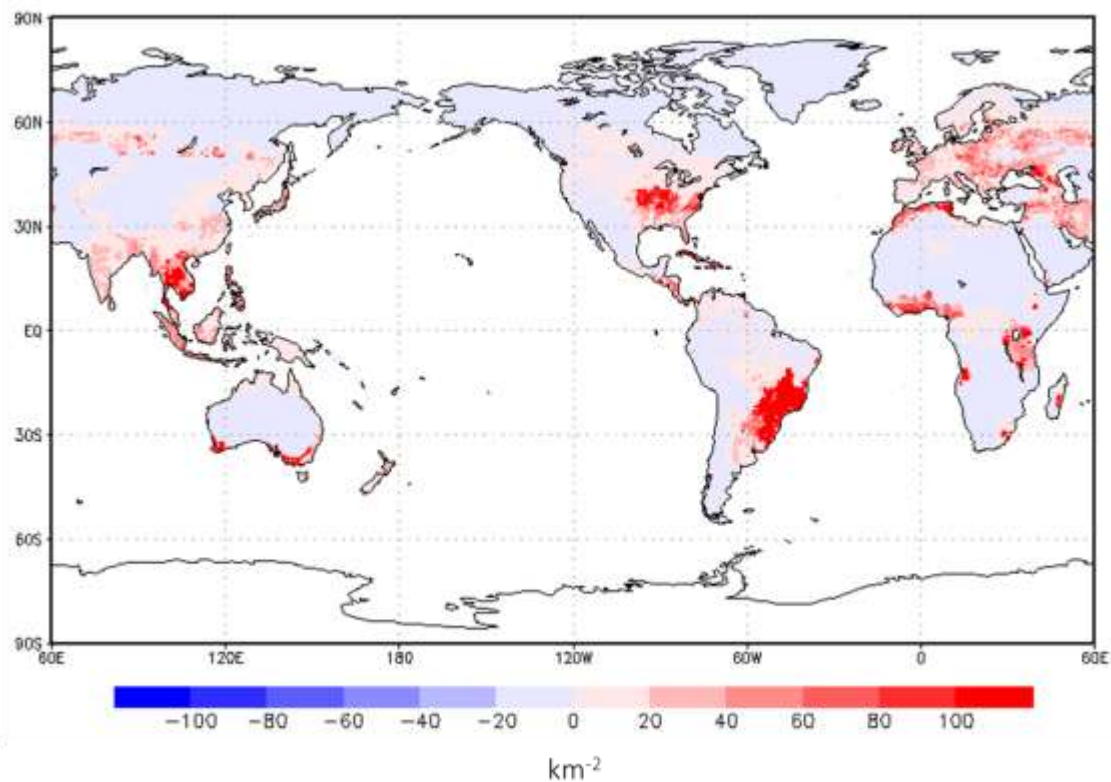


**Figure S9.** Difference between the mean bioenergy cropland area in 2050–2060 and 2030–2040 based on the LUH2 data set.

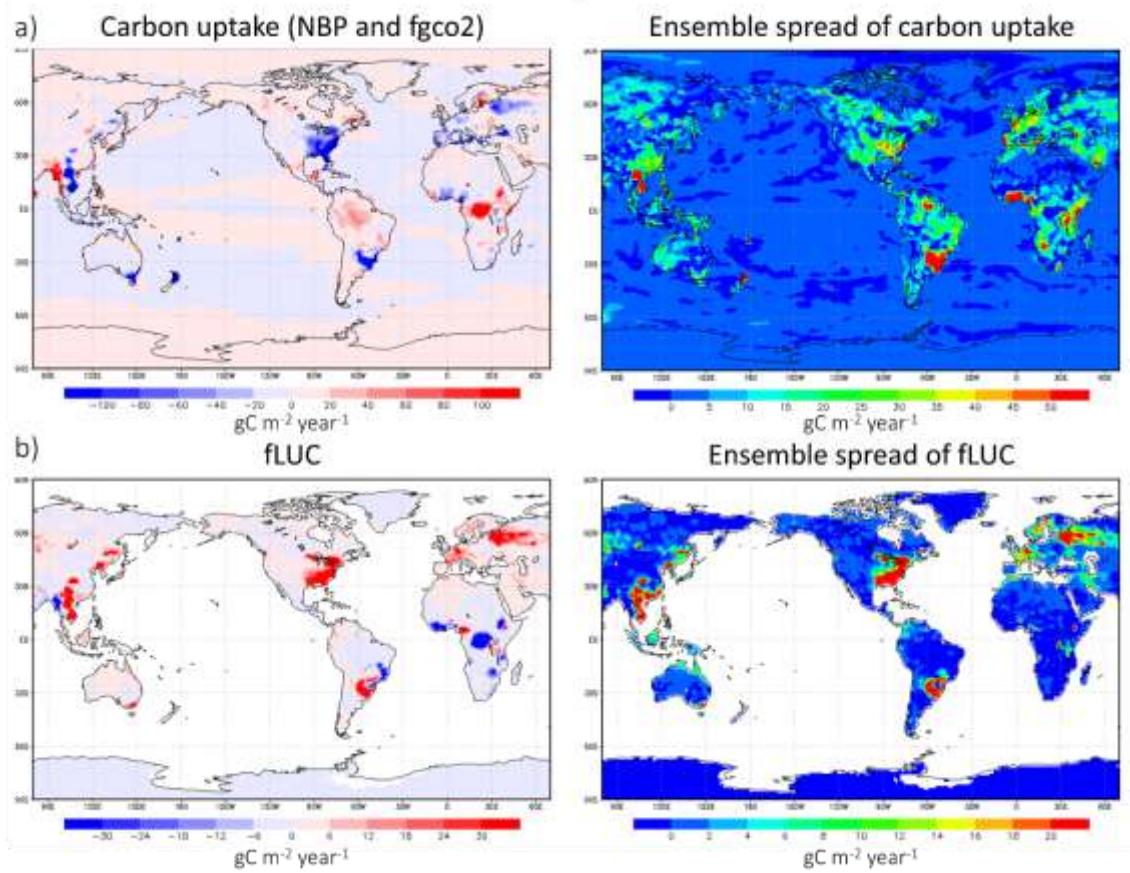


**Figure S10.** The difference in (a) the carbon uptake and (b) land-use change emissions before and after the peak of CO<sub>2</sub> concentration is shown as ensemble means of six (four for fLUC) CMIP6 ESMs.

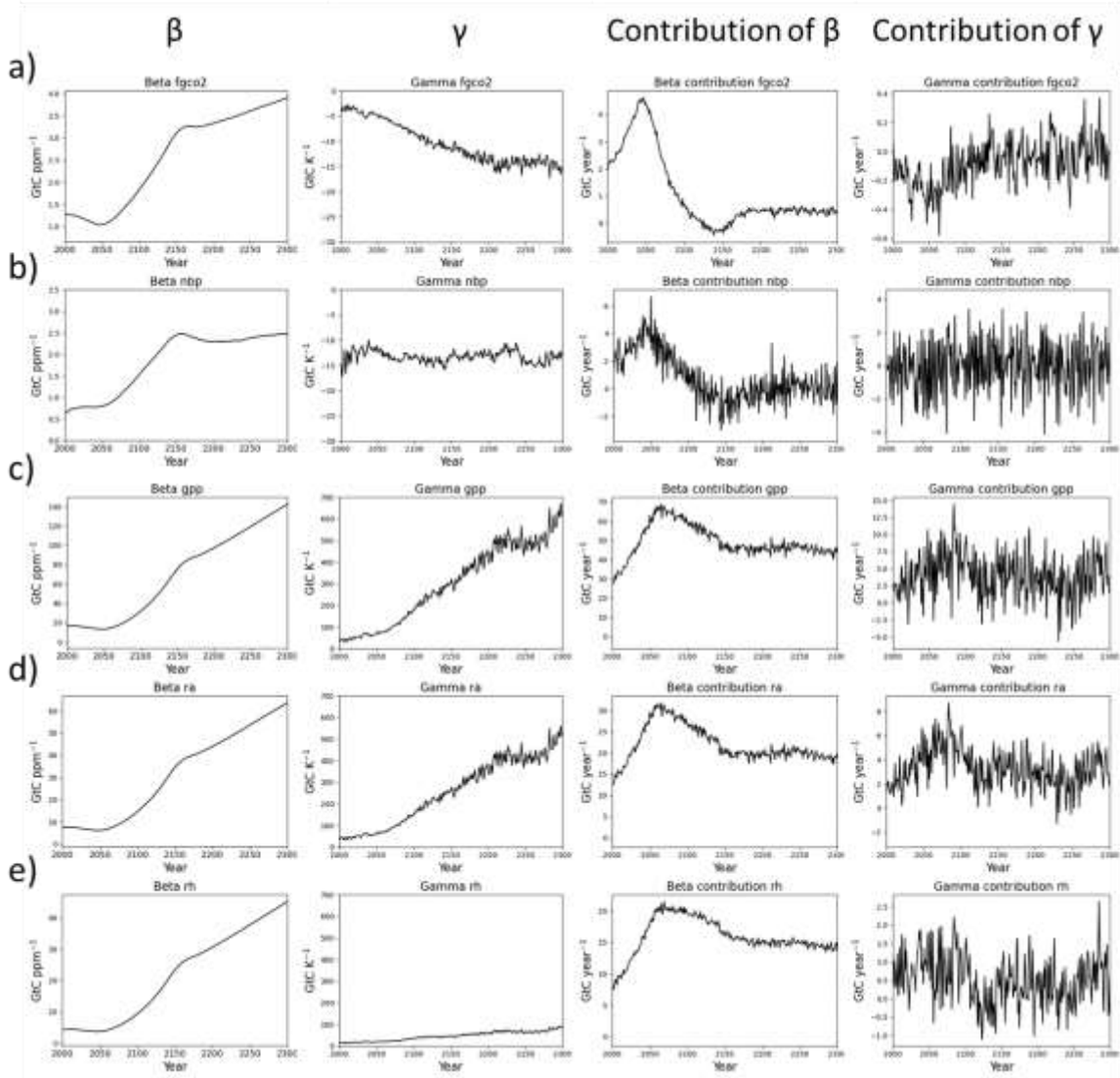


**Figure S11.** Carbon-concentration  $\beta$  (GtC ppm<sup>-1</sup>), carbon-temperature  $\gamma$  (GtC °C<sup>-1</sup>) feedback parameters and their contributions to the carbon fluxes (GtC year<sup>-1</sup>) for (a) ocean fgco2, and land (b) NBP, (c) GPP, (d) R<sub>A</sub> and (e) R<sub>H</sub> as a function of time (year) extended till the year 2300 for IPSL-CM6A-LR under the SSP5-3.4-OS pathway.



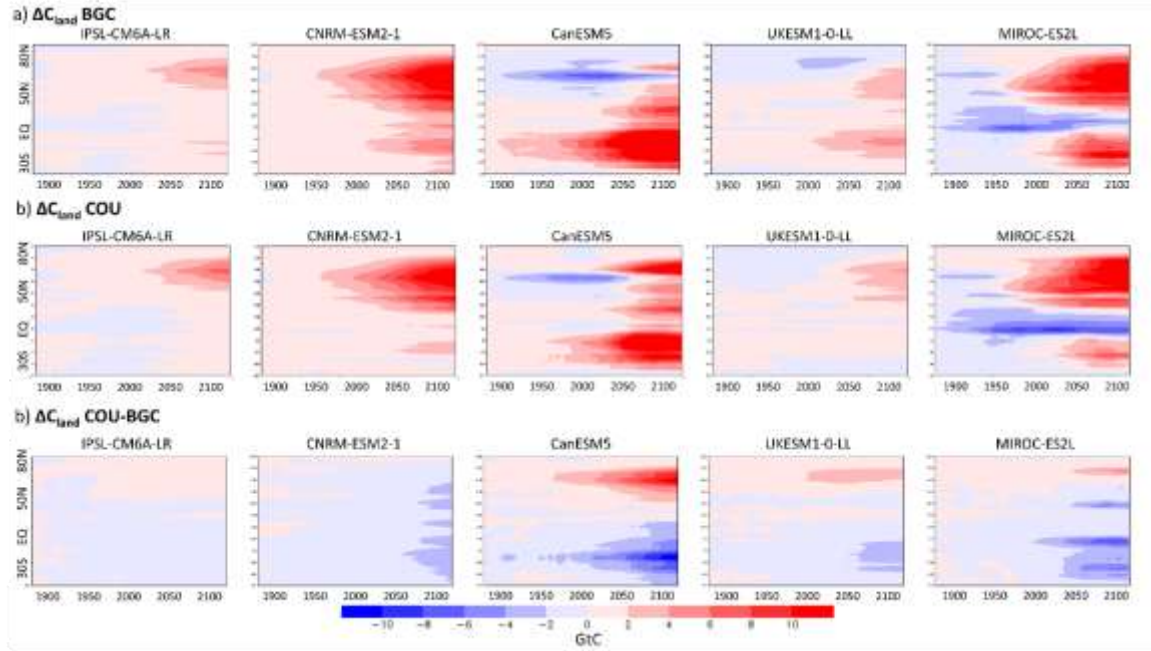


**Figure S12.** The spatiotemporal variation of zonal cumulative land carbon pool (positive to land) in (a) BGC simulation, (b) COU simulation, and (c) COU-BGC difference.

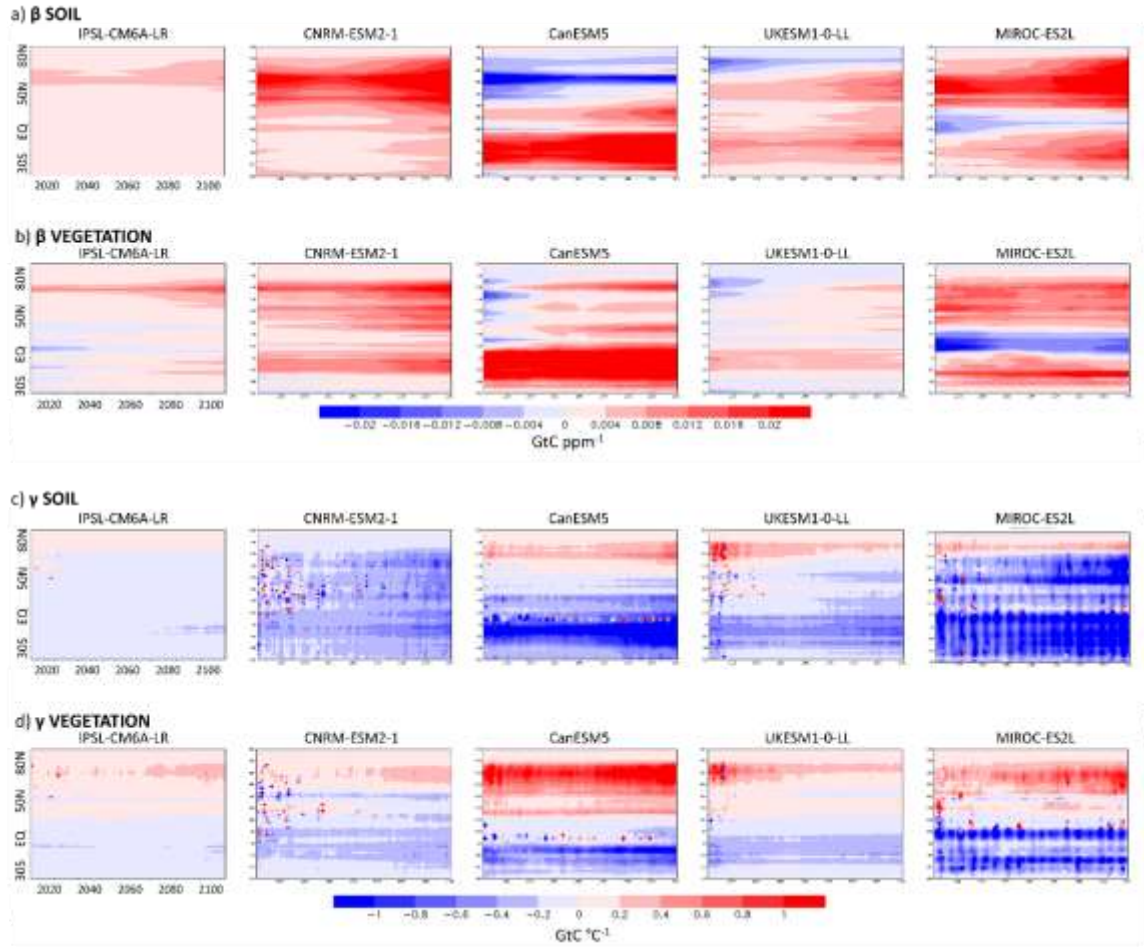


**Figure S13.** The spatiotemporal variation of zonal cumulative (a)  $\beta_{\text{soil}}$ , (b)  $\beta_{\text{veg}}$  (GtC ppm<sup>-1</sup>), (c)  $\gamma_{\text{soil}}$  and (d)  $\gamma_{\text{veg}}$  (GtC °C<sup>-1</sup>) calculated from corresponding land carbon pools. Positive values indicate a net sink.

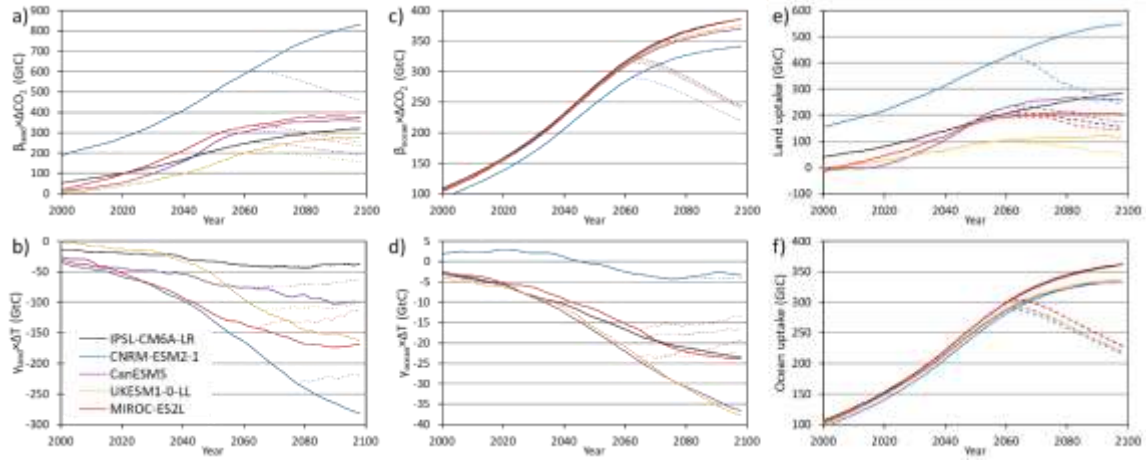


**Figure S14.** Contributions of carbon-concentration  $\beta$  and carbon-temperature  $\gamma$  feedback parameter to the cumulative carbon fluxes (GtC) under the SSP5-3.4-OS pathway. Panel (a) shows the contribution of  $\beta_{\text{land}}$ , (b) of  $\gamma_{\text{land}}$ , (c)  $\beta_{\text{ocean}}$ , and (d) of  $\gamma_{\text{ocean}}$ . Panels (e) and (f) show cumulative uptakes by land and ocean, respectively. Solid lines indicate this study and dashed lines – an experiment with the  $\beta$  and  $\gamma$  fixed as means of the five years corresponding to the peak of  $\text{CO}_2$  concentration (2060-2065) and temperature (vary among models). Here, all calculations are based on the smoothed data by using a 5-year moving average.



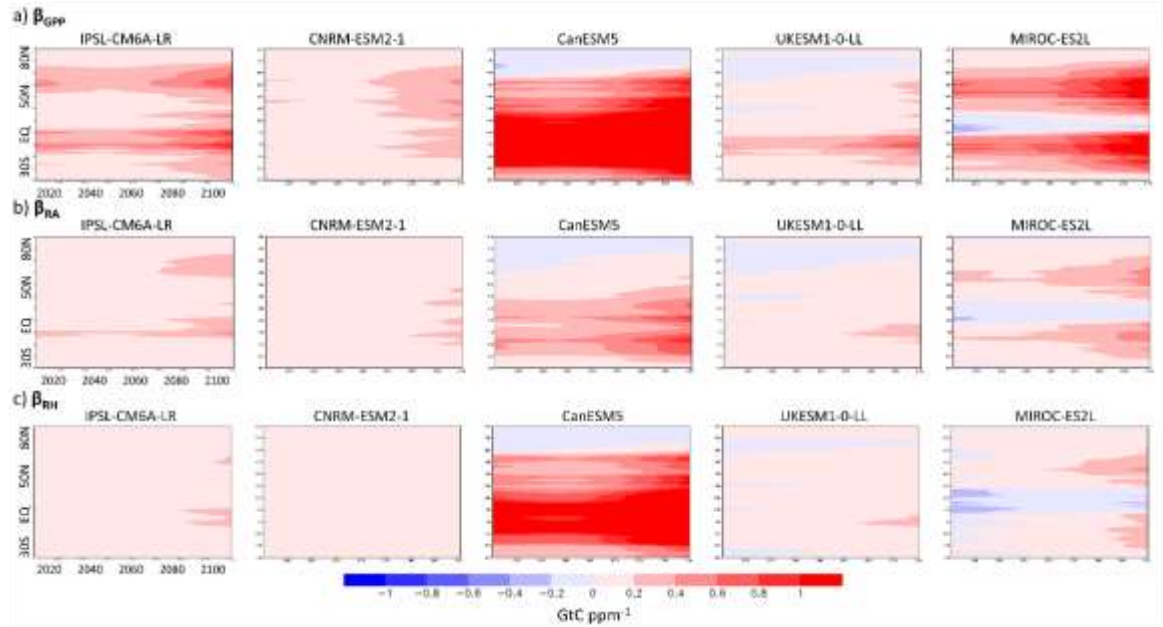


**Figure S15.** The spatiotemporal variation of zonal cumulative (a)  $\beta_{GPP}$ , (b)  $\beta_{RA}$ , and (c)  $\beta_{RH}$  ( $\text{GtC ppm}^{-1}$ ) is calculated from corresponding cumulative land carbon fluxes. Positive values indicate a net sink for  $\beta_{GPP}$  and a net source for  $\beta_{RA}$  and  $\beta_{RH}$ .

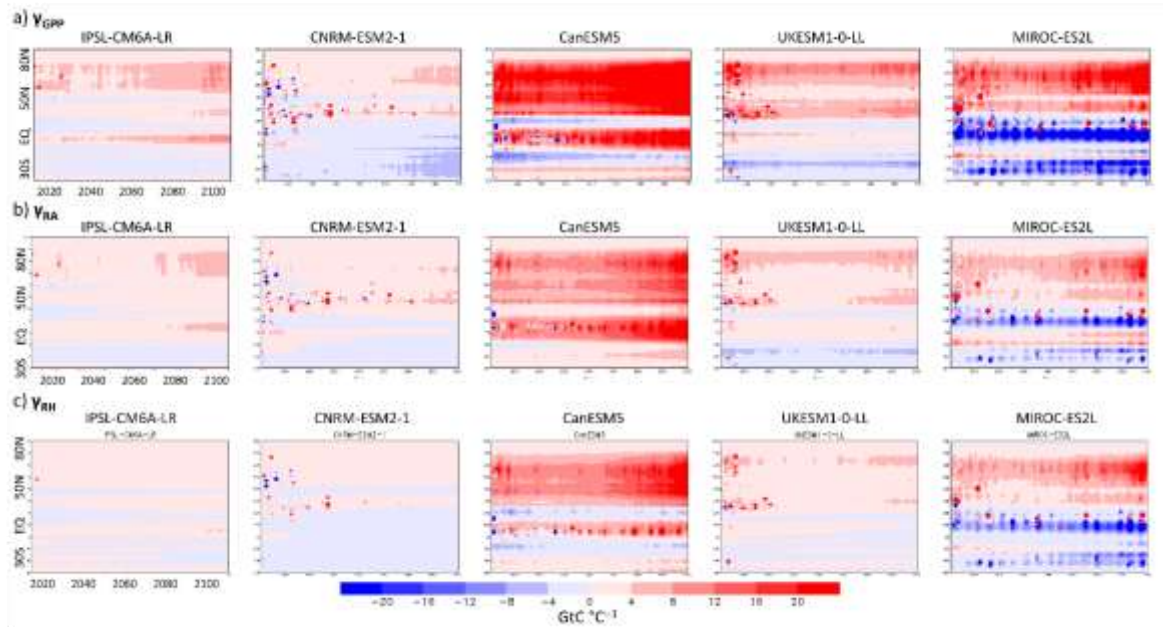


**Figure S16.** The spatiotemporal variation of zonal cumulative (a)  $\gamma_{GPP}$ , (b)  $\gamma_{RA}$ , and (c)  $\gamma_{RH}$  ( $\text{GtC } ^\circ\text{C}^{-1}$ ) calculated from corresponding cumulative land carbon fluxes. Positive values indicate a net sink for  $\gamma_{GPP}$  and a net source for  $\gamma_{RA}$  and  $\gamma_{RH}$ .